Bistable phase control via rocking in a nonlinear electronic oscillator

Javier M. Buldú[1,2], K. Staliunas[1,3], J.A. Casals[1], Jordi Garcia-Ojalvo[1]
[1] *Departament de Física i Enginyeria Nuclear, Universitat Politècnica de Catalunya, Colom 11, 08222 Terrassa, Spain.*
[2] *Nonlinear Dynamics and Chaos Group, Departamento de Física Aplicada y Ciencias de la Naturaleza, Universidad Rey Juan Carlos, Tulipán s/n, 28933 Móstoles, Madrid, Spain.*
[3] *Institució Catalana de Recerca i Estudis Avançats (ICREA), Colom 11, E-08222 Terrassa, Barcelona, Spain.*

We experimentally demonstrate the effective rocking of a nonlinear electronic circuit operating in a periodic regime. Namely, we show that driving a Chua circuit with a periodic signal, whose phase alternates (also periodically) in time, we lock the oscillation frequency of the circuit to that of the driving signal, and its phase to one of two possible values shifted by π, and lying between the alternating phases of the input signal. In this way, we show that a rocked nonlinear oscillator displays phase bistability. We interpret the experimental results via a theoretical analysis of rocking on a simple oscillator model, based on a normal form description (complex Landau equation) of the rocked Hopf bifurcation.

PACS numbers: 05.45.-a

I. INTRODUCTION

Multistability is a very useful property of nonlinear systems, which lends itself to relevant applications such as memory storage and pattern recognition [1]. An intriguing version of the phenomenon that can take place in nonlinear oscillators is that of phase bistability, whereby the phase of the oscillator can lock to one of two possible values for a given set of operating conditions. Since the two states differ only in phase but not in amplitude, phase bistability provides a way of storing digital information without involving abrupt changes in average energies.

The phase of most nonlinear oscillators is invariant, i.e. the system is indifferent to arbitrary variations of the phase. A standard way of forcing a nonlinear oscillator to have a fixed phase is by phase locking. This procedure consists simply on forcing the nonlinear oscillator with a harmonic signal whose frequency is close to its natural frequency. In those conditions, the system may lock its frequency and phase to that of the external driving. A constant phase difference arises between the injected signal and the system output, which depends on the frequency mismatch, injection strength and internal parameters of the system [2]. Obviously, phase locking leads to a monostable phase response of the system.

Recently, a phase locking procedure was proposed that leads to a bistable phase response [3]. The method, called *rocking*, relies on subjecting the driving (harmonic) signal to an additional modulation (e.g. a sinusoidal modulation of its amplitude). In this situation, the phase of the output oscillations can still lock to that of the input signal, but (somewhat counterintuitively) with a $\pm\pi/2$-shift relative to the input phase. In other words, the oscillator locks its phase to one of two values shifted by π, which results in a bistable response: for a given set of parameter values (including the parameters of the driving signal), the system can be forced to oscillate in one of two different regimes depending on the initial condition.

Rocking was initially proposed in the context of broad-area lasers [3], where transverse patterns are notoriously hampered by the lack of phase bistability, in contrast with other well-known optical systems. In this context, rocking has been experimentally shown to lead to stable patterns in lasers [4]. This is the only experimental demonstration so far of the rocking phenomenon. However, rocking is a general physical phenomenon, and should exist in any self-oscillating system [5]. Here we demonstrate for the first time the rocking effect in a nonlinear electronic oscillator. Additionally, in contrast with the initial theoretical proposal [3], where the secondary modulation of the driving field was sinusoidal (resulting in a bichromatic master signal), here we use a periodic alternation of the phase of the input signal, keeping its amplitude constant. Our results show that rocking can be efficiently attained in an electronic system under these conditions.

The paper is organized as follows. Experiments are described in Sec. II. Section III contains a theoretical analysis in terms of the normal form of the Hopf bifurcation, which takes the form of a complex Landau equation (CLE) with periodic injection.

II. EXPERIMENTAL OBSERVATIONS

Our nonlinear electronic oscillator is the so-called Chua circuit, which is a simple electronic circuit widely used for the generation of low dimensional chaotic regimes [6]. In this article we investigate the behavior of the Chua circuit operating in a periodic regime. The oscillator is driven by a periodic external signal (with frequency close to the characteristic frequency of the circuit) whose phase alternates periodically in time.

Figure 1 shows a detailed description of the Chua circuit used in this paper. A nonlinear resistor is connected to a set of passive electronic components. We have systematically studied the dynamical ranges of the Chua

circuit when $R_{\rm exc}$ is varied, observing stable, periodic, excitable and chaotic dynamics. We fix the circuit to have a periodic output by setting $R_{\rm exc} = 1.957$ kΩ. Under these conditions the dynamics of the circuit lies on a limit cycle with natural frequency $f_0 = 2840.5$ Hz (see Fig. 2). The build-up time of these oscillations (time interval necessary for the oscillation amplitude to grow a factor e starting from the off state) is, for the experimental parameters chosen, around 15 ms.

We use an external voltage source (of amplitude $V_{\rm ext}$) in order to perturb the circuit. External input is introduced into the circuit through a voltage follower and a coupling resistance $R_{\rm coup}$, which can be tuned in order to modify the coupling strength.

The dynamics of the circuit is described by the equations:

$$C_1 \frac{dV_1}{dt} = \frac{V_2 - V_1}{R_{\rm exc}} - g(V_1, V_{cc}) + \frac{V_{\rm ext} - V_1}{R_{\rm coup}} \quad (1a)$$

$$C_2 \frac{dV_2}{dt} = \frac{V_1 - V_2}{R_{\rm exc}} + I_L \quad (1b)$$

$$L \frac{dI_L}{dt} = -V_2 - R_L I_L \, . \quad (1c)$$

Hence the phase space of this system is three-dimensional. $g(V_1, V_{cc})$ is a piecewise-linear function given by:

$$g(V_1, V_{cc}) = G_a V_1 + 0.5(G_a - G_b)(|V_1 + B_p| - |V_1 - B_p|) \, . \quad (2)$$

Here G_a, G_b are the slopes and $\pm B_p$ denote a break point [7].

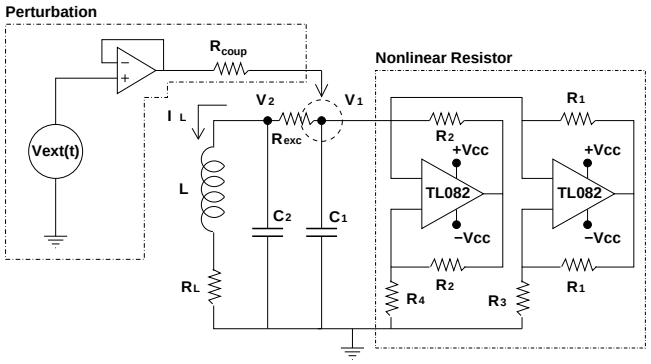

FIG. 1: Scheme of the electronic oscillator used in this paper. The circuit is built with two TL082 operational amplifiers, and with passive electronic components of values: $C_1 = 10$ nF, $C_2 = 100$ nF, $L = 8$ mH, $R_1 = 10$ $k\Omega$, $R_2 = 270$ Ω, $R_3 = 1$ $k\Omega$, $R_4 = 220$ Ω, $R_L = 20$ Ω. Operational amplifiers are fed by a DC source of $V_{cc} = \pm 9.0$ V. We set $R_{\rm exc} = 1.957$ $k\Omega$ in order to have periodic dynamics when the circuit is isolated. The coupling resistance is $R_{\rm coup} = 22$ $k\Omega$. V_1 and V_2 correspond to the outputs of the circuit.

The phase of the limit cycle oscillations shown in Fig. 2 is not defined. It can be fixed by applying to the system

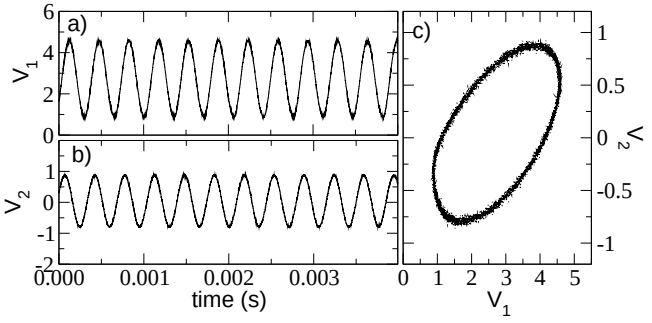

FIG. 2: Dynamics of the nonlinear circuit in the absence of external input. Time traces of V_1 (a) and V_2 (b), and the corresponding phase space plot (c).

a periodic signal of frequency $f_{\rm ext}$ and amplitude $V_{\rm ext}$. Figure 3 shows the locking region of the system in the parameter space defined by the amplitude and frequency of the external forcing. As expected, a resonance exists at the natural frequency of the circuit, $f_0 = 2840.5$ Hz.

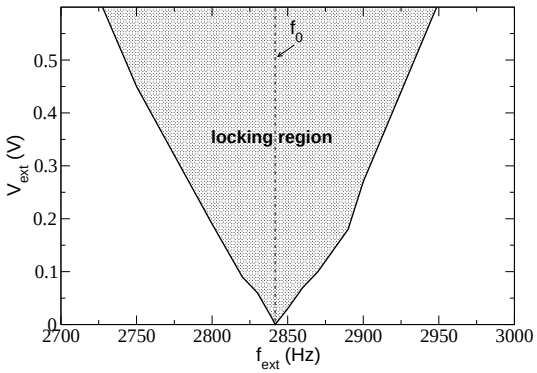

FIG. 3: Response of the system to an external periodic input. $f_0 = 2840.5$ Hz corresponds to the natural frequency of the circuit.

The single-frequency forcing described in the previous paragraph locks the phase to a *unique* value with a well-defined shift with respect to the input signal. Nevertheless, as mentioned above, a bistable phase response can be obtained by *rocking* the oscillator. To that end, we perturb the harmonic forcing by introducing periodic π-jumps in the phase, with frequency $f_{\rm jump}$. Figure 4(a) displays the power spectrum of the input signal, which differs from a pure sinusoidal perturbation in the fact that now it exhibits two maxima at frequencies $f_{\rm ext}^{(1)}$ and $f_{\rm ext}^{(2)}$, centered around a frequency $f_{\rm ext}$ and separated by an amount that we denote $f_{\rm jump}$. In the particular experimental conditions of Fig. 4, $f_{\rm ext} = 2830$ Hz and $f_{\rm jump} = 94.33$ Hz. The inset shows the corresponding time series, where a jump of π in the frequency can be observed. Plots 4(b,c,d) show the response of the circuit for low, intermediate and high amplitudes of the external input, respectively. Specifically, we can observe an entrainment to $f_{\rm ext}^{(1)}$ for low couplings, a shift to $f_{\rm ext}$ for

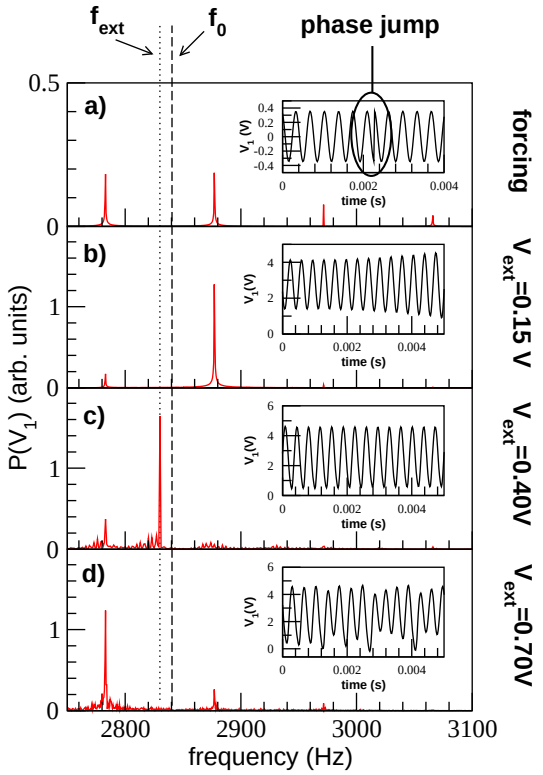

FIG. 4: Response of the circuit to a periodic signal of frequency $f_{\rm ext} = 2830$ Hz, amplitude $V_{\rm ext}$ (variable), and jumps of π in the phase with a frequency $f_{\rm jump} = 94.33$ Hz. In (a), we plot the power spectrum and the temporal evolution (inset) of the external signal. (b), (c) and (d) show the power spectra and the time series (insets) for $V_{\rm ext} = 0.15$ V, $V_{\rm ext} = 0.40$ V and $V_{\rm ext} = 0.70$ V respectively.

intermediate couplings (note that this frequency is not present at spectrum of the external input), and finally, an entrainment to $f^{(2)}_{\rm ext}$ when the coupling is high enough.

The situation depicted in Fig. 4(c) constitutes an example of rocking: the system is perturbed with a periodic signal with phase jumps of π (alternating with frequency $f_{\rm jump}$), and as a result an output phase arises that is different from any of the two alternating inputs, but equal to their mean value. In other words, the system is not able to follow the phase jumps due to their relatively high frequency, and adopts a phase located between the two alternating values of the input phase. The rocking effect can be observed by comparing the spectrum of the input signal with that of the circuit. When the circuit is entrained to the frequency $f_{\rm ext}$, not present at the input spectrum, we have rocking [compare Figs. 4(a) and (c)].

We now examine the dependence of the rocking phenomenon on the amplitude and frequency of the input signal. Figure 5 shows the rocking region in the parameter plane defined by those two quantities, which is closed and surrounded by other two regions where the system is entrained to either $f^{(1)}_{\rm ext}$ or $f^{(2)}_{\rm ext}$, as we have already seen in Figs. 4(b) and (d). This result can be explained by taking into account the spectrum of the input signal, with two peaks ($f^{(1)}_{\rm ext} = f_{\rm ext} - f_{\rm jump}/2$ and $f^{(2)}_{\rm ext} = f_{\rm ext} + f_{\rm jump}/2$), and the locking region given by Fig. 3. Let us consider first a rocked input signal with a low mean frequency $f_{\rm ext}$ lying outside (on the left of) the locking region. When shifting the spectrum of the input signal (by modifying $f_{\rm ext}$) from low to high frequencies, the peak at the highest frequency ($f^{(2)}_{\rm ext}$) is the first to enter the locking region, entraining the system at $f^{(2)}_{\rm ext}$. This entrainment has a resonance at $f^{(2)}_{\rm ext} = f_0$ (or $f_{\rm ext} = f_0 - f_{\rm jump}/2$), which corresponds to the minimum observed at region A of Fig. 5.

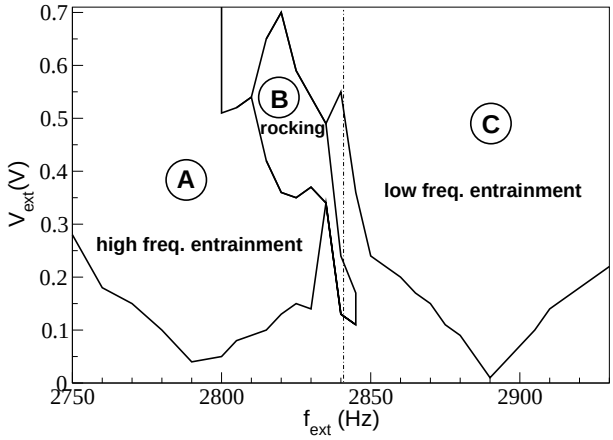

FIG. 5: Entrainment regimes in the parameter space of $f_{\rm ext}$ and $V_{\rm ext}$ for a given $f_{\rm jump} = 94.33$ Hz. The dashed line corresponds to the natural frequency of the circuit ($f_0 = 2840.50$ Hz). In the region labeled A, the circuit is entrained to $f^{(2)}_{\rm ext} = f_{\rm ext} + f_{\rm jump}/2$. Rocking is observed at region B. In region C the system is entrained to the lower frequency of the input spectrum, $f^{(1)}_{\rm ext} = f_{\rm ext} - f_{\rm jump}/2$.

A similar situation occurs when shifting the input signal from high to low frequencies from an starting point placed outside (now, at the right of) the locking region. In this case, the peak corresponding to the lower frequency $f^{(1)}_{\rm ext}$ enters first the locking region, and entrains the system to $f^{(1)}_{\rm ext}$ (region C in Fig. 5). As in the previous case, there is a resonance at $f^{(1)}_{\rm ext} = f_0$ (or $f_{\rm ext} = f_0 + f_{\rm jump}/2$). We find rocking between the two regions of entrainment, where the system is pulled from both sides and none of them has enough influence to overcome the other. The rocking region (B in Fig. 5) also shows a resonance appearing, as it would be expected, at $f_{\rm ext} = f_0$.

It is worth noting that the rocking region is closed in ($f_{\rm ext}$,$V_{\rm ext}$) space, which means that not only frequency but also amplitude must be properly tuned. Indeed: for low amplitudes, the system can not be entrained and oscillates with its natural frequency. On the other hand, when amplitude is too high, the system follows the phase jumps of the input frequency, i.e. $f^{(1)}_{\rm ext}$ and $f^{(2)}_{\rm ext}$, and rocking is not observed. Only for moderate amounts of

coupling the system is perturbed by the input signal, but not enough to follow it, laying at a frequency between $f_{\rm ext}^{(1)}$ and $f_{\rm ext}^{(2)}$. This is what we call rocking.

So far we have identified the rocked state in terms of the frequency response of the system. But as mentioned in the Introduction, and as described in the next section, two different solutions, with a phase difference of π, are possible when the system is rocked. Taking the phase of the rocked system as a reference $\phi_{\rm rock}$, the input signal, which consists of a sine wave with phase jumps of π, has a phase $\phi_{\rm ext} = \phi_{\rm rock} + \phi_0 \pm \frac{\pi}{2}$, where ϕ_0 is a certain phase difference due to the impedance of the circuit and $\pm\frac{\pi}{2}$ accounts for the phase jumps of the external signal, which occur with a frequency $f_{\rm jump}$. When $\phi_0 \sim 0$, the phase difference between the input and the output $\phi_{\rm ext} - \phi_{\rm rock}$ is $\pm\frac{\pi}{2}$. In order to distinguish experimentally between the two possible solutions of the rocked state, we proceed in the following way: starting with the circuit operating under the influence of the rocking signal, we define a reference sinusoidal signal whose frequency and phase are matched with that of the rocked output state. We then reduce the amplitude of the external signal with the aim of losing the rocking of the system. When rocking is lost, we increase again the amplitude of the external perturbation up to its initial value, in order to recover the rocking, and compare the reference sinusoidal signal with the output of the system. A possible result is shown in Fig. 6, in which (a) plots the external perturbation $V_{\rm ext}$ (in red), the reference signal $V_{\rm ref}$ (black dashed line), and the response of the circuit V_2 (black line). It can be observed that the output voltage is in phase with the reference signal, while it has a $\pm\frac{\pi}{2}$ phase difference with the input signal [compare the phase-plane plot in Fig. 6(c) with that in its inset]. It can also happen that, upon reentrance in the rocking region, the situation resembles instead that in plots (b) and (d) of Fig. 6. In that case, while the output signal keeps a $\pm\frac{\pi}{2}$ phase difference with the external perturbation [see inset in plot (d)], it is however in antiphase (i.e. has a phase difference of π) with the reference signal [see main graph in plot (d) of Fig. 6]. This fact reveals that the circuit is now operating at the other solution, which is shifted π with respect with the previous one.

Both solutions are possible and stable when the system is inside the rocking region, choice of one or another depends on the initial conditions. In spite of their stability, spontaneous jumps between the two solutions, driven by internal noise in the circuit, is possible near the border of the rocking region. The effect of noise was not investigated in detail in the present article. Further work in that direction is in progress.

III. THE NORMAL FORM DESCRIPTION

The nonlinear circuit used in the experiments described above is a self-oscillatory system, where oscillation sets in after a Hopf bifurcation [8]. Since we do not focus here on other dynamical regimes of the Chua circuit (such as bistable or chaotic regimes), then the full description [Eqs. (1a)-(1c)] is not necessary in order to understand the basic features of the phenomena reported here, and we use a theoretical description as simple as possible. This simplicity of description allows us to obtain analytical results, as well as an insight into the rocking process. The evolution of the slowly varying envelope of the oscillatory system above (but close to) the Hopf bifurcation is in a most simple way described by the Landau equation:

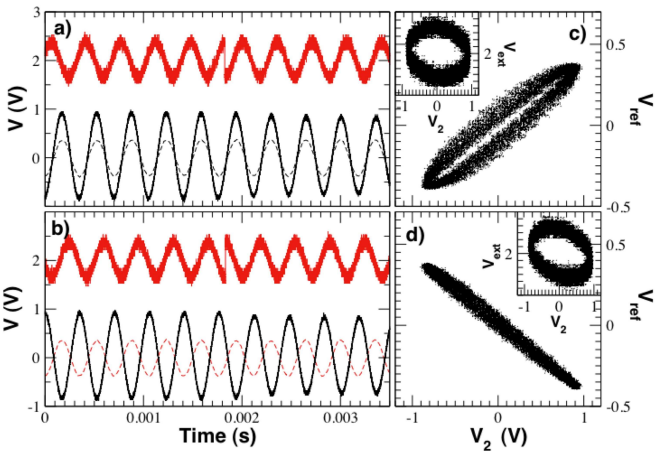

FIG. 6: Phase bistability of the rocking state. (a,b) Time series of the external perturbation $V_{\rm ext}$ (top trace), the response of the system V_2 (solid bottom trace), and a reference sinusoidal signal $V_{\rm ref}$ (solid dashed trace). (c,d) Synchronization plots in the phase plane $(V_2, V_{\rm ref})$; the insets show the corresponding plot in the plane $(V_2, V_{\rm ext})$.

$$\frac{dA}{d\tau} = A + i\Delta\omega A - |A|^2 A + A_{\rm inj}(\tau), \qquad (3)$$

here τ is a dimensionless time, normalized to the build-up time of the oscillations τ_0, which depends on the distance to the Hopf bifurcation point. In the experimental conditions described above, it is $\tau_0 = 15$ ms. The variable $A(\tau)$ denotes the slowly varying complex envelope of the variable (voltage), i.e. $V(\tau) = A(\tau)e^{i\omega_0 t} + c.c.$ with ω_0 being a reference frequency (chosen to coincide with the injection frequency). $A_{\rm inj}(\tau)$ is the envelope of the injection signal. It is generally a complex quantity, but here we will consider it, without the loss of generality, as a real-valued function. $\Delta\omega$ in Eq. (3) represents the mismatch between the oscillation frequency and the injection frequency. Equation (3) can also be derived systematically as the amplitude equation corresponding to the circuit model (1a)-(1c). To that end one can assume periodic, but slowly modulated oscillations (providing a slow temporal scale), then make a perturbative expansion and analyze the solvability of the different orders of approximation. At a certain order Eq. (3) appears.

In the resonant case ($\Delta\omega = 0$), eq. (3) is variational,

since it can be written as $dA/d\tau = -\delta V/\delta A^*$, with a potential

$$V = -|A|^2 + \frac{1}{2}|A|^4 - \mathrm{Re}(A_{\mathrm{inj}}A^*)\,. \qquad (4)$$

In the absence of injection $A_{\mathrm{inj}} = 0$, the potential has the shape of a sombrero and displays a degenerated minimum along the circumference $|A|^2 = 1$ in the complex plane Re(A)-Im(A), as shown in Fig. 7(a). In that case

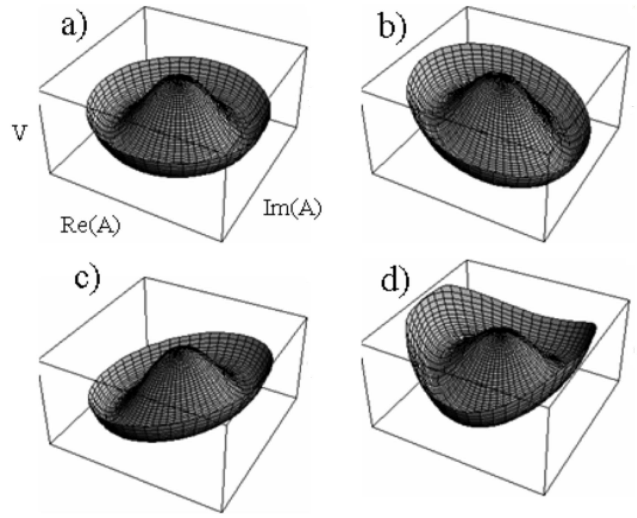

FIG. 7: Qualitative 3D plot of the potential associated with Eq. (3), which describes a rocked oscillator (arbitrary units are used). a) Without injection ($A_{\mathrm{inj}} = 0$) the potential is radially symmetric, in agreement with the phase invariance of the free running oscillator. b) With constant injection ($\Omega = 0$) the potential tilts along the direction Re(A) proportionally to the forcing amplitude F, and a single isolated minimum appears, corresponding to the phase-locked state of the oscillator with injected signal; here $A_{\mathrm{inj}} < 0$. c) Like (b), but with $A_{\mathrm{inj}} > 0$. Under rocking ($\Omega \neq 0$) the potential oscillates back and forth between the two cases b and c, through a. Under such a forcing, the system would tend to remain close to the imaginary axis Re(A) = 0, around either of the two regions separated by the local maximum around the origin. d) Effective potential associated with Eq. (9), which is the initial potential in (a), deformed due to fast rocking.

the phase of the complex envelope, $\varphi = \arg(A)$, is thus arbitrary. Alternatively, one says that Eq. (3) displays phase invariance.

In the presence of a constant resonant injection the potential is tilted along the Re(A)-axis, where it exhibits an isolated minimum. This is plotted in Figs. 7(b,c). Phase invariance is thus broken, and the phase of the output is locked to that of the input ($\varphi = 0$). In the case of an external signal with constant amplitude but periodically alternating phase, $A_{\mathrm{inj}} = A_0\ \mathrm{sign}[\sin(\Omega\tau)]$, the potential is periodically tilted, or rocked, around the axis Im(A) (hence the name "rocking" [3]). Under this rocking the system avoids active areas in the phase space Re(A)-Im(A) (located on the axis Re(A) in this case) and drifts to quiet areas (located along the axis Im(A)) [3]. The phase symmetry is again broken but now, unlike the usual case of constant forcing, the phase of the oscillations can lock to one of two values, symmetric with respect to the input phase, differing by π. In other words the radially symmetric Hopf bifurcation describing the oscillations of the autonomous system [of which Eq. (3) with $A_{\mathrm{inj}} = 0$ represents its normal form] deforms into a pitchfork bifurcation due to the rocking of the potential.

Previous studies [3] considered a harmonically oscillating input $A_{\mathrm{inj}} = A_0 \sin(\Omega\tau)$. Following the experiments described above, we investigate here instead the case of a step-like modulation $A_{\mathrm{inj}} = A_0\ \mathrm{sign}[\sin(\Omega\tau)]$. In the analytical study we consider the limit of "strong and fast" rocking $A_0 = \epsilon^{-1}f$, $\Omega = \epsilon^{-1}\omega$, $(0 < \epsilon << 1)$, and keep the rest of parameters as $O(1)$ quantities. This allows us to separate the slow time scale τ of the unforced system and the fast time scale $T = \epsilon^{-1}\tau$ of rocking: $\partial_\tau \to \epsilon^{-1}\partial_T + \partial_\tau$. We seek for a solution to Eq (3) of the form $A(\tau) = a(\tau) + \xi(T) + \mathcal{O}(\epsilon)$, which means that we separate the order parameter into a fast oscillating part $\xi(T)$ (due to the rocking) and a slowly varying part $a(T)$. At order ϵ^{-1} we find:

$$\frac{d\xi}{dT} = A_{\mathrm{inj}}(T), \qquad (5)$$

leading to

$$\xi(T) = \int A_{\mathrm{inj}}(T)dT + \mathrm{const}, \qquad (6)$$

Assuming that the choice of integration constant results in $\langle\xi\rangle = 0$, the integration yields $\langle|\xi|^2\xi\rangle = 0$, and $\langle|\xi|^2\rangle = \langle\xi^2\rangle = \gamma$, with $\gamma = (A_0/\Omega)^2\pi^2/12 \approx (A_0/\Omega)^2 0.82247$. Next we integrate Eq. (3) [with the *Ansatz* for $A(\tau)$ given above] over the forcing period, and consider that the slow amplitude does not change sensibly over one period:

$$\frac{da}{d\tau} = a - (|a|^2 a + a^*\langle\xi^2\rangle + 2a\langle|\xi|^2\rangle) + i\Delta\omega a\,, \quad (7)$$

where we have used the fact that the averages of odd powers of ξ are zero, as mentioned above, $\langle\xi\rangle = 0$, $\langle|\xi|^2\xi\rangle = 0$. Inserting the calculated averages of the even powers of ξ yields:

$$\frac{da}{dt} = (1-2\gamma)a + \gamma a^* + |a|^2 a + i\Delta\omega a\,. \qquad (8)$$

This expression differs from that in [3] only in the coefficient γ, equal to $\gamma = \frac{1}{2}(A_0/\Omega)^2$ in that case, where the input signal was harmonic.

In the fully resonant limit $\Delta\omega = 0$, Eq. (8) is variational, and its potential reads

$$V = -(1-2\gamma)|a|^2 + \frac{1}{2}|a|^4 - \gamma\frac{1}{2}\left(a^2 + a^{*2}\right)\,. \qquad (9)$$

A comparison with the potential (4) of Eq. (3) reveals that the effect of rocking consists in deforming the rotationally symmetric potential of the undriven system,

so that now local minima appear at $a = \pm i\sqrt{1-\gamma}$, corresponding to two symmetric points located at the axis $\mathrm{Im}(a)$. These minima correspond to the steady solutions of Eq. (8) in the resonant case. The deformation of the potential is compatible with the general theory of motion in rapidly oscillating fields [9].

Equation (8) has two relevant spatially homogeneous solutions (apart from the trivial one $a = 0$):

$$\begin{aligned} a &= \pm u \exp(i\phi) \\ u^2 &= 1 - 2\gamma + \sqrt{\gamma^2 - \Delta\omega^2} \\ \phi &= -\frac{1}{2}\arcsin(\Delta\omega/\gamma), \end{aligned} \tag{10}$$

of equal intensities but opposite phases. The existence range of these "rocked states" is

$$|\Delta\omega| < \gamma < \frac{1}{3}(2 + \sqrt{1 - 3\Delta\omega^2}), \tag{11}$$

as follows from the analysis of relations (10). In particular the condition $\sqrt{3}\Delta\omega < 1$ is required. The analytical estimate of the locking range given by Eq. (11) is plotted as solid lines in Figs. 8 and 9. The entrainment

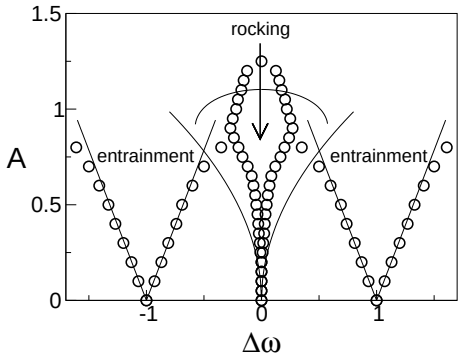

FIG. 8: Rocking range of a perturbed oscillator, as obtained theoretically from Eq. (11) and (12) (solid lines) and by numerical integration of Eq. (3) (white circles), for a rocking frequency $\Omega = 1$.

range has been evaluated considering only one harmonic component of the driving signal (the one closest to resonance), and solving Eq. (3) with $A_{\mathrm{inj}}(\tau) = A_0 \exp(i\Omega\tau)$. The locking boundary is then given by $A_0 = \mid \Omega - \Delta\omega \mid$, as a simple analysis of Eq. (3) shows. For a step-like injection $A_{\mathrm{inj}} = A_0\ \mathrm{sign}[\sin(\Omega\tau)]$, the rocking condition reads

$$A_0 = \mathrm{mod}(\Omega - \Delta\omega)\frac{\pi}{2}. \tag{12}$$

A physical interpretation of both the lower and upper rocking conditions in Eq. (11) is as follows. For relatively large amplitudes of rocking, $A_0 > A_0^{\max}(\Omega)$, the slow component of the oscillations $a(t)$ decays to zero and one is left with the fast oscillating component of the amplitude. Therefore, in that case the amplitude of the oscillations follows adiabatically the oscillations of the

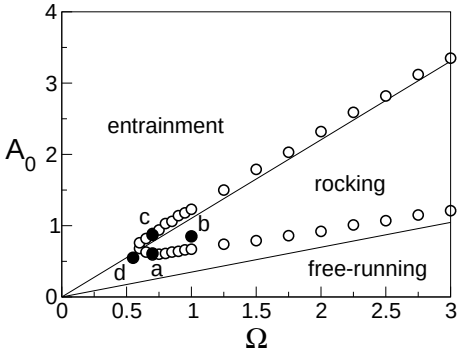

FIG. 9: Rocking range of a perturbed oscillator, as obtained theoretically from Eq. (11) (solid lines) and by numerical integration of Eq. (3) (white circles), for a detuning $\Delta\omega = 0.1$. Black circles denote points whose trajectories are shown in Fig. 10 below. In the entrainment region the oscillator follows adiabatically the input signal, while in the rocking region the phase is set to the solutions obtained in Eq. (10).

driving force. On the other hand, for small values of the rocking amplitude, $A_0 < A_0^{\min}(\Omega)$, the phase of the oscillator is unlocked from that of the driving force, and evolves freely.

We integrated numerically, by means of a second order Runge-Kutta scheme, the complex Landau equation (3), in order to verify the evaluated rocking ranges. The rocking area was indeed found to decrease with increasing detuning $\Delta\omega$, as depicted by the white circles in Fig. 8. Increasing the frequency of rocking Ω also leads to an increase of the rocking range, as depicted in 9. Both behaviors are in qualitative and quantitative agreement with the analytical result given by Eq. (11).

The different dynamical regimes observed in our numerical calculations are summarized in Fig. 10, which shows typical phase trajectories on the complex plane of the oscillation amplitude. Locking corresponds to closed trajectories, which are placed symmetrically with respect to the $\mathrm{Re}(A)$-axis. Besides the periodic regimes displayed in Figs. 10(b,c), more complicated ones were also found in the locking area (predominantly at its border), such as period doubled and chaotic orbits. Examples of these behaviors are given in plots (a) and (d) of Fig. 10.

IV. CONCLUSIONS

We have provided for the first time experimental evidence of the phenomenon known as rocking in a nonlinear electronic oscillator. Rocking allows the control of the oscillation phase, which furthermore takes the form of a bistable response: in the presence of a harmonic driving whose phase is periodically inverted in time (at a much smaller frequency than that of the carrier oscillations), the system responds with one of two phases orthogonal to the input phase. Coexistence of these two phases can be revealed by multiple entrances into the locking region,

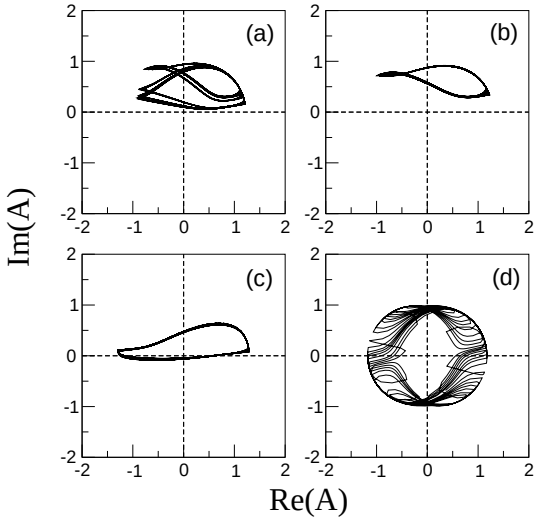

FIG. 10: Trajectories in phase space for the situations depicted as black circles in Fig. 9 above. Plots (a-c) correspond to the rocking regime: (a) lies on the boundary with the free-running regime, (b) lies deep within the rocking region, and (c) is located on the boundary with the adiabatic regime. (d) lies outside the rocking regime. Parameter values are $\Delta\omega = 0.1$ and: (a) $\Omega = 0.7$, $A_0 = 0.61$, (b) $\Omega = 1.0$, $A_0 = 0.85$, (c) $\Omega = 0.7$, $A_0 = 0.87$, and (d) $\Omega = 0.55$, $A_0 = 0.45$.

and can occur spontaneously in the boundaries.

The basic properties of the rocking (phase bistability and transition to the adiabatic and free-running regimes) can be well understood in terms of normal form analysis, i.e. by investigating the rocked Hopf bifurcation by means of the complex Landau equation description (3)-(11). There are some quantitative discrepancies, especially at large amplitudes of the external drive, when the normal form description (valid close to threshold) no more holds. Also it seems (see Figs. 3 and 5) that the Chua oscillator displays a weak nonlinear resonance (i.e. the resonance frequency depends on the oscillation amplitude) that is not considered in the normal form description (3). Those specific aspects of rocking could be observed by modelling the full equations (1)-(2) of the circuit.

These results could provide a means to encode information in phase-based communication systems.

Acknowledgments

Discussions with Germán J. de Valcárcel are acknowledged. This work was financially supported by the Ministerio de Educación y Ciencia (Spain) through projects BFM2003-07850, FIS2005-07931-C03-03, and TEC2005-07799, and by the Generalitat de Catalunya.

[1] J. Foss, A. Longtin, B. Mensour, and J. Milton, Phys. Rev. Lett. **76**, 708 (1996).
[2] A. Pikovsky, M. Rosenblum, and J. Kurths, *Synchronization: A universal concept in nonlinear sciences* (Cambridge University Press, 2001).
[3] G. J. de Valcárcel and K. Staliunas, Phys. Rev. E **67**, 026604 (2003).
[4] A. E. Martin, M. M. Quesada, V. B. Taranenko, E. Roldan, and G. J. de Valcarcel, Phys. Rev. Lett., in press (2006).
[5] G. J. de Valcarcel, arXiv.org:nlin/0207004 (2002).
[6] R. N. Madan, *Chua's Circuit: A Paradigm for Chaos* (World Scientific, Singapore, 1993).
[7] M. Kennedy, IEEE Trans. Circuits Sys. I:Fund Theor. and Appl. **40**, 657 (1993).
[8] J. L. Moiola and L. O. Chua, Int. J. Bifurc. Chaos **9**, 295 (1999).
[9] L. D. Landau and E. M. Lifschitz, *Course of Theoretical Physics, vol. 1* (Pergamon, London, 1959).